JACS Au
AN OPEN ACCESS JOURNAL OF THE AMERICAN CHEMICAL SOCIETY

pubs.acs.org/jacsau

Perspective

Shaping the Structure and Response of Surface-Grafted Polymer Brushes via the Molecular Weight Distribution

Jacinta C. Conrad* and Megan L. Robertson*

Cite This: *JACS Au* 2023, 3, 333−343

Read Online

ACCESS | Metrics & More | Article Recommendations

ABSTRACT: Breadth in the molecular weight distribution is an inherent feature of synthetic polymer systems. While in the past this was typically considered as an unavoidable consequence of polymer synthesis, multiple recent studies have shown that tailoring the molecular weight distribution can alter the properties of polymer brushes grafted to surfaces. In this Perspective, we describe recent advances in synthetic methods to control the molecular weight distribution of surface-grafted polymers and highlight studies that reveal how shaping this distribution can generate novel or enhanced functionality in these materials.

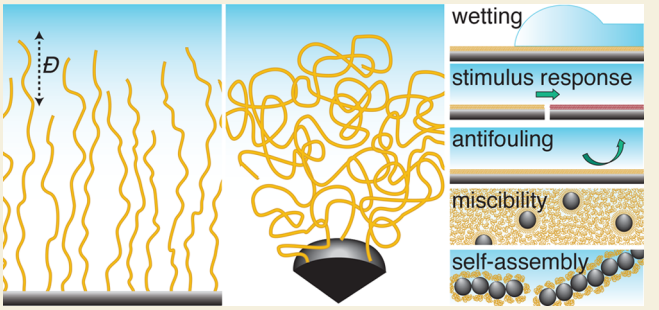

KEYWORDS: *surface-grafted polymer, dispersity, molecular weight distribution, polymer-grafted nanoparticle, polymer conformation, stimulus response*

INTRODUCTION

Polymer brushes are an increasingly used route to generate soft, functional surfaces for applications in sustainable energy conversion and storage,[1] sensing,[2] and separations.[3] In a polymer brush, one end of the polymer is tethered to a substrate via a covalent bond. Even a short brush, of thickness no more than a few nanometers, can dramatically modify the surface properties. For example, attaching a polymer brush to a surface can alter the surface wettability,[4−6] tethering a zwitterionic polymer bearing both positive and negative charges can render a surface very low-fouling to proteins,[7] and grafting a polymer that undergoes a stimulus-dependent conformational change (in response to, for example, light, solution pH, or salt concentration and valency) can render a surface "smart"[8] (i.e., stimulus responsive) and even replicate functions of biological systems.[9]

Because the tether restricts the states available to the polymer, the conformations of polymers in brushes can markedly differ from those in solution. On a planar substrate, solvated brushes adopt "mushroom" conformations that are close to those in solution when the areal grafting density σ is low (Figure 1(a)), and the average brush height h scales with the number of monomers N as $h \sim N^{3/5}$. When the grafting density becomes comparable to the radius of gyration R_g of the polymer in solution, however, solvated chains experience (pairwise) excluded volume interactions with neighboring monomers. Competition between these excluded volume interactions and the polymer elasticity drives chains to become stretched orthogonally to the surface, leading to a "semidilute" brush whose height scales[10,11] with both N and σ as $h \sim N^1\sigma^{1/3}$ (Figure 1(b)). Further increasing the grafting density leads to a "concentrated" brush whose height scales[10,11] as $h \sim N^1\sigma^{1/2}$ (Figure 1(c)). Here, the $\sigma^{1/2}$ scaling reflects higher-order interactions among the monomers.

Brushes grafted to the curved surface of a spherical nanoparticle also undergo a transition from mushroom to semidilute to concentrated as the grafting density at the particle surface is increased (Figure 1(d−f)). Unlike planar brushes, however, the crowding from the polymers decreases away from the particle surface due to the curvature. Thus, spherical polymer brushes exhibit scaling behaviors distinct from those of planar brushes. In the semidilute regime, $h \sim (N^1\sigma^{1/3})^{3/5}$ (refs 13, 14). Brushes at high grafting densities transition from concentrated (near the brush surface) to semidilute (at the periphery) if they are sufficiently long (at distances greater than a critical radius r_c (ref 15)), and $h \sim (N^1\sigma^{1/2})^x$ with $3/5 \leq x \leq 1$ by analogy to flat brushes (refs 10, 11).

These scaling relationships, however, are for the average brush height and do not account for an inherent feature of synthetic polymer systems: their molecular weight distribution. The number-average molecular weight $M_n = \sum_{i=1}^{\infty} x_i M_i$ and weight-average molecular weight $M_w = \sum_{i=1}^{\infty} w_i M_i$, where x_i and w_i are,

Received: November 22, 2022
Revised: January 17, 2023
Accepted: January 18, 2023
Published: February 6, 2023

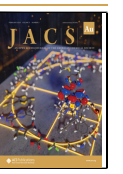

https://doi.org/10.1021/jacsau.2c00638
JACS Au 2023, 3, 333−343

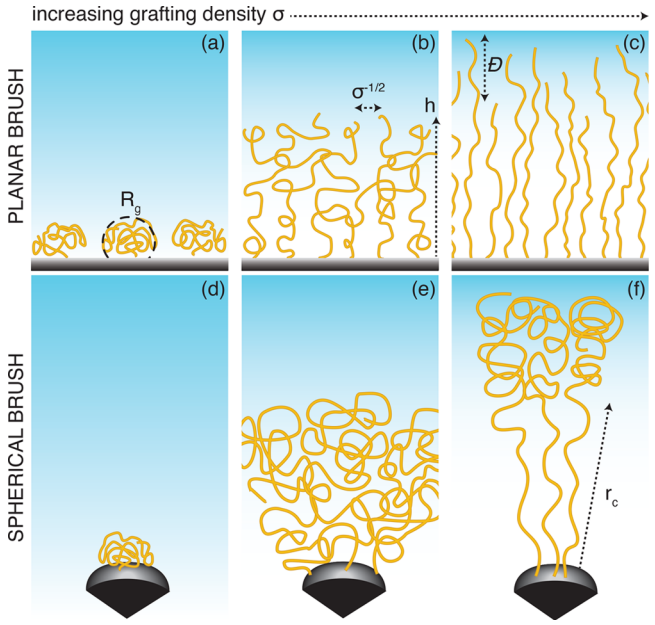

Figure 1. Schematic illustration of the conformation of (a–c) planar and (d–f) spherical polymer brushes with increasing grafting density σ. The polymer radius of gyration R_g, brush height h, and (for spherical brushes) critical radius r_c are shown. The dispersity $Đ$ is the ratio of the weight-average and number-average molecular weights. Panels d–f are adapted with permission from ref 12. Copyright 2010 American Chemical Society.

respectively, the number fraction and weight fraction of polymers with molecular weight M_i, do not typically coincide in synthetic polymers. Thus, for most synthetic polymers with a unimodal distribution, the dispersity $Đ = M_w/M_n \geq 1$; moreover, surface-grown polymer brushes are more disperse than polymers synthesized concurrently in solution.[16] For polymers with a unimodal molecular weight distribution, $Đ$ (previously reported as PDI) is also directly related to the breadth of the molecular weight distribution, as $Đ = (s/M_n)^2 + 1$, where s is the standard deviation. (For bimodal or multimodal molecular weight distributions, the dispersity is not related to the breadth.) Whereas the effects of dispersity on the properties of polymers in the melt or solution phase have been long investigated,[17−21] recent studies have demonstrated new ways to control brush dispersity and thereby to explore its effects on functional properties.

In this Perspective, we highlight novel functionality in polymer-brush-grafted surfaces imparted through control over the molecular weight distribution. First, we describe recent advances in synthetic methods to control the dispersity of surface-grafted polymers (as opposed to polymers in solution). Then we summarize selected studies that reveal how modulating the molecular weight distribution can generate or enhance function in these soft interfaces, largely but not exclusively focusing on homopolymer systems. This focus is complementary to that of detailed reviews and perspectives on bidisperse mixed brush systems.[22,23] Finally, we highlight avenues to develop the fundamental understanding required to generate novel surface function by shaping the molecular weight distribution of surface-grafted polymers.

SYNTHETIC METHODS TO CONTROL BRUSH DISPERSITY

There has been significant interest in developing synthetic methods to alter not only the breadth but also the shape of polymer molecular weight distributions.[24−32] These methods offer exquisite control over the molecular weight distribution. Many of these methods, however, are not applicable to surface-tethered polymer chains, due to use of techniques such as metered addition of initiator[24,25] and flow reactors in which narrowly dispersed samples accumulate in the vessel to build a targeted molecular weight distribution[29] or the mixing of polymers of narrow size range.[33] Furthermore, quantification of the molecular weight distribution of surface-grafted chains offers additional challenges[34] due to insufficient mass of polymer present on the surface (such as on planar surfaces), preventing use of standard techniques such as gel permeation chromatography; instead, polymers must be chemically cleaved from the surface prior to characterization. Nonetheless, prior studies have carefully compared the molecular weight distribution of surface-grafted chains and those polymerized in solution, noting important differences: even in the case of targeting the synthesis of low dispersity polymers, the surface-tethered chains exhibited a bimodal distribution and were of higher dispersity than those in solution.[16]

Recent articles have reviewed the state-of-the-art in synthesis methods for tailoring the molecular weight distribution of polymer brushes.[27,35,36] Techniques for synthesizing polymer brushes generally fall within two categories: grafting-to and grafting-from reactions, which each have their own advantages and drawbacks.[37,38] In grafting-to reactions, preformed polymers are grafted to the functionalized surface. In this approach, a variety of methods could in theory be employed to vary the breadth and shape of the molecular weight distribution[24,26−29] if the chain ends retain the required functionality for grafting to the surface; the grafting density obtained via this method, though, is typically low. By contrast, higher grafting densities are obtained through grafting-from techniques, in which the initiator is first attached to the surface, followed by polymerization from the surface-tethered initiator. As noted above, however, methods of varying the breadth and shape of the molecular weight distribution are limited.

Reversible deactivation radical polymerizations (RDRP, i.e. "controlled" or "living" radical polymerizations) are often employed in surface-initiated polymerizations, due to the diversity of monomer types that can be synthesized via these techniques, convenience of surface attachment of the required initiators, mild reaction conditions, and ease of obtaining relatively low dispersity ($Đ \sim 1.1-1.2$) polymers. More recently, methods to tune dispersity in these polymerizations have been explored. In surface-initiated atom-transfer radical polymerization (ATRP), reduction of catalyst concentration,[39] reduction of surface initiator concentration,[40] addition of a reducing agent,[40] and addition of a terminating agent[41] have increased the dispersity. A bimodal distribution could also be obtained through methods such as partial deactivation of chain ends.[42] In surface-initiated reversible addition−fragmentation chain-transfer (RAFT) polymerization, bidisperse/bimodal brushes have been produced by[43] (i) attaching a RAFT initiator, (ii) synthesizing a surface-grafted polymer, (iii) cleaving the RAFT agent from the chain ends, (iv) attaching a second RAFT agent, and (v) synthesizing a second polymer brush of differing molecular weight from the first. Additionally, brushes

https://doi.org/10.1021/jacsau.2c00638
JACS Au 2023, 3, 333−343

with side-chain dispersity (as opposed to the traditional main-chain dispersity) have been synthesized through RAFT techniques.[44] Organocatalyzed living radical polymerizations have also been used to synthesize brushes of varying dispersity, through temperature-selective radical generation[45] and also through exploitation of simultaneous polymerization and chain-end substitution in the presence of sodium azide.[46] Few existing studies report surface-initiated polymerizations of tunable dispersity that go beyond the use of RDRP; one notable example is the application of ring-opening polymerization in the presence of transesterification.[47] Though much progress has been made in synthetic techniques to produce surface-grafted polymers of varying breadth in the molecular weight distribution , additional effort is required to apply recent advances in control over shape of the molecular weight distribution to surface-grafted chains.

ENHANCING PROPERTIES BY INCREASING DISPERSITY

Planar Brushes

Polymer Conformation. Theoretical studies using self-consistent field theory (SCFT) have revealed that the conformation of polymers grafted to flat surfaces is greatly altered by dispersity. Increasing the polymer dispersity increased the brush thickness and changed the shape of the density profile from convex to concave.[48] Theory and Monte Carlo simulations confirmed this shape change and moreover showed that even small dispersity could suppress chain-end fluctuations and that the hydrodynamic penetration length generally increased with dispersity.[49] For the case of bimodal brushes in which the length difference was varied, increasing the length difference at fixed total grafting density led to extended density profiles with two parts; the structure of the inner part (containing the ends of the short chains) did not depend on the length or fraction (at constant grafting density) of the long chains.[50] The long brushes in a bimodal molecular weight distribution were stretched near the grafted surface, such that the longer chain ends were localized near the brush periphery.[51] Densely grafted disperse chains adopted a "crown and stem" conformation, in which the polymers closest to the substrate (at higher grafting density) were stretched by interactions with neighboring chains; chains at the brush periphery, by contrast, were less extended and collapsed.[52] These results were supported by Monte Carlo simulations, which confirmed that the short and long chains in a bimodal brush were vertically segregated due to chain stretching.[53,54]

Early experimental studies to probe dispersity effects employed bidisperse brushes (containing two different size polymers). Neutron reflectivity experiments on highly asymmetric poly(dimethylsiloxane)-polystyrene (PDMS−PS) diblock copolymers, for which the PDMS blocks were grafted to the surface and the PS blocks dangled into a good solvent, showed that the larger PS blocks were stretched by the presence of shorter PS blocks.[55] The conformation of these brushes was well predicted by lattice-based self-consistent mean field theory.[56] Likewise, neutron reflectivity experiments on bidisperse polystyrene brushes in a good solvent, toluene, found that longer chains were vertically stratified near the brush periphery (Figure 2(a,b)),[57] as predicted by SCFT. In the melt limit (for which solvent did not penetrate the brush), bidisperse polyisoprene brushes in chloroform−ethanol mixtures also exhibited a stratified structure.[58] Although the density profile

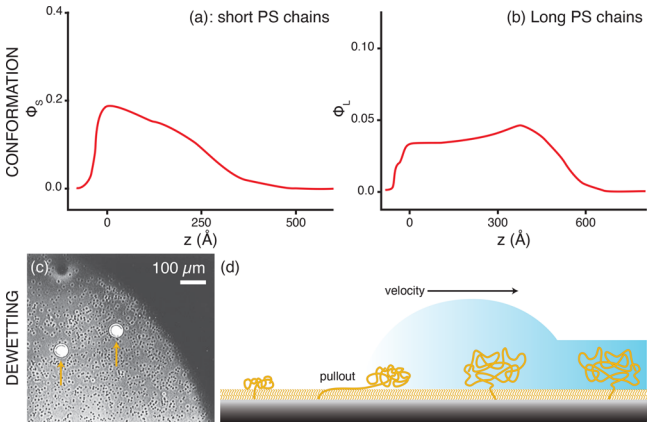

Figure 2. Bidisperse brushes exhibit distinct conformation and functional properties. (a, b) Volume fraction of (a) short and (b) long PS chains as a function of the distance from the substrate in a polystyrene brush anchored by P2VP (short chain: deuterated 0.52×10^5 Da; long chains: 1.03×10^5 Da) in toluene, a good solvent. Adapted with permission from ref 57. Copyright 1998 American Chemical Society. (c, d) Long chains suppress autophobic dewetting in polymer films. (c) Optical micrograph of two typical cylindrical holes (indicated by the arrows) in a 900 Å thick polystyrene film on a 66 Å thick polystyrene brush after 8 min of annealing at 175 °C. Reproduced with permission from ref 60. Copyright 1996 American Chemical Society. (d) Schematic illustration of a moving rim of a thin film on a polymer brush, in which the capillary forces driving the motion compete against the force required to pull out the long polymer chains. Adapted with permission from ref 61. Copyright 1996 EDP Sciences.

measured with neutron reflectivity was not well described by the SCFT model of ref 48, a modified lattice-based self-consistent mean field theory approach provided closer agreement.[59]

SCFT has also been used to explore the structure of mixed binary brushes in which the solvent selectivity differed for two chemically distinct polymers. When the molecular weights of the two brush polymers were equal, the polymers phase separated such that the outer layer preferred the solvent.[62,63] For bimodal brushes of long and short chains, however, two layered structures could form: one in which the outer layer was in its good solvent, and one in which the long chains (in their poor solvent) covered a layer of the short chains. When the fraction of short chains was low, these chains underwent a transition from a "coil" state (buried deep inside the brush) to a "flower" state (stretched at the periphery).[55] Thus, the bimodal size distribution offers opportunities for generating switchable surfaces with a discontinuous phase transition.

Wetting and Miscibility. Thin polymer layers or films on surfaces are often unstable. Grafting a polymer brush to the surface can reduce the unfavorable enthalpic interactions that promote dewetting of the polymer film (Figure 2(c)); nevertheless, entropic interactions may still drive dewetting. Experiments showed that adding long brush molecules to a polystyrene brush could suppress this autophobic dewetting (depicted schematically in Figure 2(d)). SCFT calculations also confirmed that bidisperse brushes could eliminate dewetting,[64] with fewer long brushes needed to suppress the dewetting as the bidispersity was increased. These SCFT calculations also indicated that the long chains reduced the entropic interfacial tension between the brush and free polymer interface.

Segregation. The phase behavior of binary disperse brushes grafted to a planar substrate depends on many parameters, including the grafting density σ, the grafting ratio (the ratio of

https://doi.org/10.1021/jacsau.2c00638
JACS Au 2023, 3, 333−343

the numbers of grafted chains of each species), and the asymmetry in the chain length; the latter two parameters are related to the bidispersity. When the polymers are immiscible, polymers constrained by surface tethers can phase separate laterally and/or vertically, leading to a variety of morphologies. These included a "layered" structure (in which one component vertically segregated to the substrate), a "rippled" state (in which the components laterally segregated), and "dimpled" or "micelle" states (in which lateral and vertical segregation both occurred).[65,66] Mean field simulations revealed that the morphology of a given system depended on the grafting ratio[67] and hence on the bidispersity.

Much experimental work exploring the effects of molecular weight distributions has focused on characterizing the conformation of binary bidisperse brushes with distinct solvent affinities. As one example, the morphology of binary mixed brushes of PS and poly(2-vinylpyridine) (P2VP) exposed to selective solvents depended on the asymmetry of the molecular weights (or chain lengths). When the chain length asymmetry was small, the brushes segregated both laterally and perpendicularly; increasing the asymmetry in chain length drove a transition from laterally segregated domains to a layered structure, tunable through the solvent selectivity.[68] Similarly, both the surface structure of mixed brushes of poly(*N*-isopropylacrylamide) (PNIPAM) and PS in toluene (selective for PS) and its reorganization upon exposure to water−methanol (selective for PNIPAM) depended on the chain asymmetry.[69] A more recent example used PMMA and PS brushes grafted at equal (high) densities to show that the transition from disorder to ripple to cylinder followed the phase behavior predicted from Monte Carlo simulations.[70]

Stimulus Response. Many studies have explored the responsive properties of bidisperse mixed polymer brushes.[23] Such brushes, composed of two distinct polymers with different properties (such as solvent selectivity or temperature or pH response), can exhibit tunable responses. For example, the thickness, refractive index, and contact angle of mixed PAA/P2VP brushes varied with pH[71] due to the formation of layers. At extreme pH values, the charged polymer (P2VP at low pH and PAA at high pH) stretched away from the substrate due to electrostatic repulsions, whereas the other polymer was collapsed and located near the substrate. As a second example, the ability of mixed PAA/poly(ethylene oxide) (PEO) brushes[72] to adsorb and, when rinsed with salt solutions, desorb three proteins (human serum albumin, lysozyme, and fibrinogen) depended on the brush composition: PAA was required to adsorb lysozyme and fibrinogen, whereas a minimum PEO density was needed to release the proteins.[73] The responsive properties of these and similar systems, however, arise from the use of two (or more polymers).

By contrast, the effects of dispersity on the response of homopolymer brushes is less studied. Our groups posited that changes in the homopolymer polymer conformation with dispersity would alter their functional properties. First, we examined the pH-dependent response of PAA brushes of various molecular weights at constant grafting density.[74] Brushes exhibited a hysteric memory in the water contact angle around a decreasing-then-increasing pH cycle, with the contact angle upon pH decrease less than that upon pH increase. The extent of hysteresis, quantified as the difference in the pK_a values extracted from the contact angle measurements upon decreasing and increasing pH (ΔpK_a), increased as a function of brush length and dispersity (Figure 3(a)). In our original ATRP synthesis,

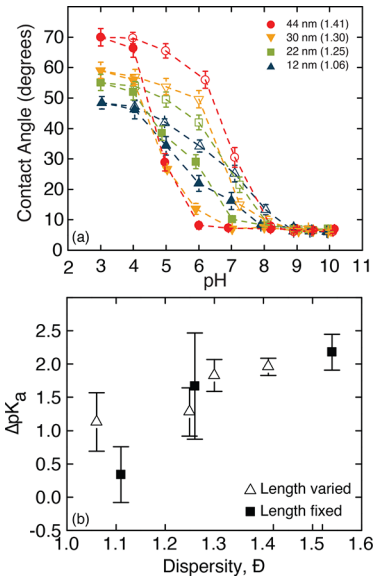

Figure 3. (a) Static contact angle as a function of pH upon decreasing (solid symbols) and increasing (open symbols) pH for PAA brushes of various lengths and dispersities. (b) Difference in the pK_a for increasing and decreasing pH (ΔpK_a) as a function of brush dispersity $Đ$. The solid symbols indicate a series of brushes for which the length was fixed; the open symbols indicate a series of brushes for which both length and dispersity were varied. Reproduced from ref 74. Copyright 2016 Royal Society of Chemistry.

however, brush dispersity increased concomitant with polymer molecular weight, hindering understanding of the driving physics. Other groups have reported hysteresis in stimulus-dependent conformation and/or response in surface-grafted weak polyelectrolytes on planar (PAA, poly(2-(diethylamino)-ethyl methacrylate) (PDEA))[75] and curved (PAA)[76] surfaces. This hysteresis has been attributed to the difference in ionization of charged groups near the brush periphery and near the substrate[77] and to formation of transient, metastable hydrogen-bonded networks.[76] To decouple the effects of increasing length and dispersity, we developed a synthetic method to increase brush dispersity in ATRP through addition of a chain terminating agent, phenyl hydrazine.[41] This approach allowed us to produce a series of brushes of near-constant length (and molecular weight) but varying dispersity. We found that ΔpK_a increased with $Đ$ when brush length was held constant, confirming that the hysteretic response was controlled in part by the dispersity (Figure 3(b)).

Antifouling. The effect of brush dispersity on the ability to repel particles was investigated using SCFT. For a single particle, the particle size determined the effect of brush dispersity on repellency. Small particles (e.g., proteins, whose radius $R \sim 1/\sqrt{2}$) readily penetrated disperse brushes, so that uniform brushes best repelled these particles. By contrast, large particles such as a bacterium or colloid (for which the radius $R \rightarrow \infty$) were less able to compress brushes of high than low dispersity; thus, disperse brushes were better able to prevent adsorption of large particles.[78] To control adsorption of biological particles,[79] both unimodal[80] and bimodal[81] mixed brushes have been designed.

In a contrasting approach, we showed that stimulus-induced changes in the conformation of disperse surface-grafted brushes could be used to tune the antifouling properties.[82] We monitored the attachment (at low pH) and detachment (at

https://doi.org/10.1021/jacsau.2c00638
JACS Au 2023, 3, 333−343

high pH, after triggering the swelling of brushes) of *Staphylococcus epidermidis* bacteria on PAA-grafted substrates. The average length of the polymer brushes controlled bacterial attachment, which was not affected by brush dispersity (Figure 4(a,b)). A minimum in surface coverage at an intermediate

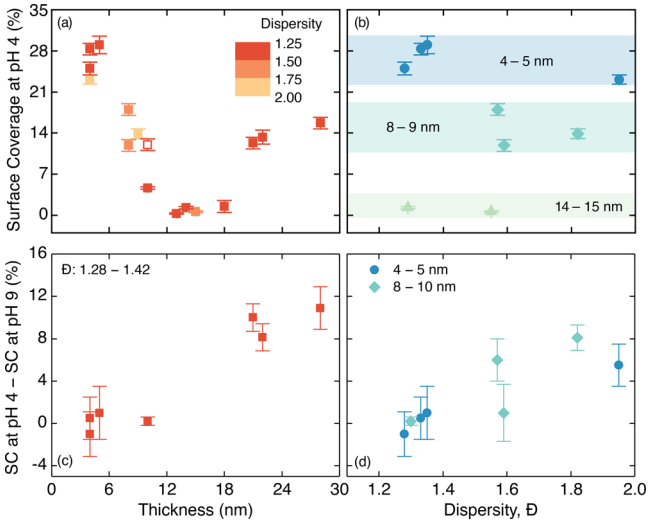

Figure 4. (a, b) Attachment of *Staphyloccocus epidermidis* bacteria on PAA brushes (at pH = 4, quantified as the percentage of the surface covered by bacteria) as a function of (a) dry brush thickness and (b) brush dispersity. (c, d) Detachment, quantified as the difference in the percentage of surface coverage at pH 5 and pH 9, as a function of (c) dry brush thickness and (d) brush dispersity. Adapted with permission from ref 82. Copyright 2017 American Chemical Society.

brush thickness arose from the competition between steric repulsions (strong for short polymer chains) and hydrophobic attractions (strong for long chains). Triggering the brush response by increasing the pH led to detachment of some bacteria. In striking contrast to attachment, which was controlled only by brush length, increasing either the brush length or dispersity enhanced detachment (Figure 4(c,d)). Thus, tailoring the molecular weight distribution of the brushes offers the possibility of orthogonally controlling attachment and detachment of adherent particles.

Spherical Brushes

Polymer Conformation. Monte Carlo simulations coupled with Polymer Reference Interaction Site Model (PRISM) calculations applied to bimodal homopolymer brushes revealed differences in polymer conformation as compared to uniformly disperse brushes. When the number of grafted short and long polymers were equal, at low to medium grafting density the radius of gyration R_g of the short polymers was lower than that in a monodisperse brush, allowing the long brushes to maximize configurational entropy. The R_g of long polymers, however, was unaltered at low grafting densities but lower (i.e., less stretched) at intermediate grafting densities.[83] Similar computational methods applied to disperse homopolymer brushes revealed that, for brushes of high dispersity, chains shorter than the number-average chain length N_n were more compressed but those longer than N_n stretched less than in a spherical brush with uniform dispersity.[84] Overall, the changes in polymer conformation in a disperse brush caused the thickness of the grafted layer to increase with dispersity (Figure 5(a,b)).

Experimentally, the length of high-dispersity ($Đ > 2.3$) poly(caprolactone) (PCL) brushes with a continuous molecular weight distribution grafted to silica nanoparticles depended strongly on $Đ$.[47] The length of three series of brushes at three grafting densities (0.21 to 0.61 chains nm^{-2}), synthesized via a ring-opening polymerization and measured through dynamic light scattering (DLS), scaled differently with the brush molecular weight (Figure 5(c)): the scaling exponent (i.e., $l_b \sim N^{\nu}$) increased concomitant with grafting density. Moreover, $\nu > 1$, counter to expectations for brushes in the concentrated regime. The differences in chain extension as l_b increased and/or σ decreased were attributed to increased hydrodynamic friction, as the brushes transitioned from nondraining to freely draining.

Inspired by these results, we set out to understand the effects of dispersity on brush conformation. We synthesized poly(*tert*-butyl acrylate) (P*t*BA) brushes via ATRP and added phenyl hydrazine to tune the dispersity between 1.03 and 1.98.[85] The brush length l_b, measured through DLS, exhibited distinct dependencies on $Đ$ in different ranges of N_w: at high N_w, l_b was

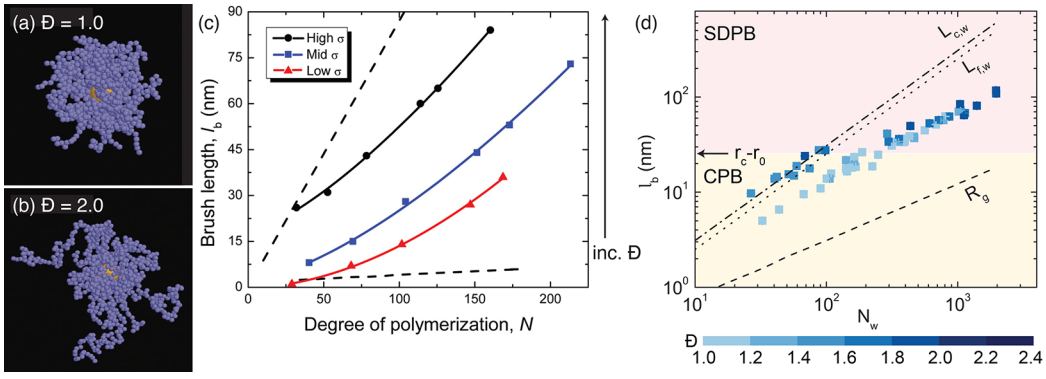

Figure 5. Brush length depends on dispersity. (a, b) Representative conformations from molecular dynamics simulations of brushes with $Đ$ of (a) 1.0 (uniform) and (b) 2.0. Panel a is reproduced with permission from ref 84. Copyright 2012 John Wiley and Sons. (c) Brush length l_b as a function of the degree of polymerization N for PCL brushes with various grafting densities (high σ: 0.61 chains nm^{-2}; mid σ: 0.43 chains nm^{-2}; low σ: 0.21 chains nm^{-2}). The upper and lower dashed lines indicate the contour length L and radius of gyration R_g, respectively. Panel c is reproduced with permission from ref 47. Copyright 2017 American Chemical Society. (d) Brush length l_b as a function of the weight-average degree of polymerization N_w for P*t*BA brushes of various $Đ$, as indicated by the color bar. The dash-dot line indicates the full length of a linear P*t*BA chain $L_{c,w}$; the dotted line indicates the length of the all-trans configuration of a P*t*BA chain $L_{f,w}$; the dashed line indicates R_g. The arrow indicates the boundary between the semidilute and concentrated brush regimes calculated from theory. Panel d is reproduced with permission from ref 85. Copyright 2021 American Chemical Society.

https://doi.org/10.1021/jacsau.2c00638
JACS Au 2023, 3, 333−343

independent of Đ, whereas at low N_w, l_b fell onto a bifurcated curve with separate branches for brushes of low and high Đ. The brush length at the onset of the bifurcation coincided with r_c, the critical length at which the brush conformation transitions from semidilute to concentrated (Figure 5(d)).

Upon separating the brushes into semidilute and concentrated regimes, we found that the length of semidilute P*t*BA brushes of varying dispersity collapsed onto a master curve as a function of the predicted scaling parameter $N_w\sigma^{1/3}$ along with semidilute brushes of PS[12] and poly(ethylene oxide-*block*-propylene oxide-*block*-ethylene oxide) triblock copolymer (PEO-*b*-PPO-*b*-PEO)[86] (Figure 6(a)). The length of concentrated brushes as a function of $N_w\sigma^{1/2}$, however, followed a bifurcated curve for our P*t*BA brushes as well as those of PMMA,[15] PS,[12] and PCL[47] (Figure 6(b)). The dispersity demarcating the low- and high-regimes was not constant across the polymers and depended on the monomer size and grafting density. Intriguingly, the boundary between the low- and high-dispersity regime was consistent with results from molecular dynamics simulations[84] indicating that dispersity effects on brush conformation were negligible above a critical grafting density or degree of polymerization.

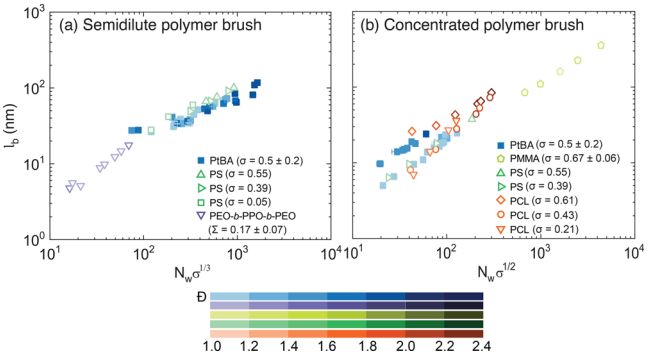

Figure 6. Brush length l_b as a function of (a) the scaled weight-average molecular weight $N_w\sigma^{1/3}$ in the semidilute polymer brush regime and (b) $N_w\sigma^{1/2}$ in the concentrated polymer brush regime, in which the color shading indicates Đ. Colors indicate series of data on various spherical brushes taken from different sources: blue: P*t*BA-grafted silica nanoparticles (Đ = 1.03−1.98, σ = 0.5 ± 0.2 chains nm^{-2}, ref 85); green: PS-grafted silica nanoparticles (Đ = 1.05−1.13, σ = 0.05−0.55 chains nm^{-2}, ref 12); yellow: PMMA (Đ = 1.19−1.28, σ = 0.59−0.73 chains nm^{-2}, ref 15); purple: PEO-*b*-PPO-*b*-PEO adsorbed silica nanoparticles (Đ = 1.10−1.20, brush adsorbed amount Σ = 0.11−0.30 chains nm^{-2}, ref 86); orange: PCL-grafted silica nanoparticles (Đ = 1.42−2.39, σ = 0.21−0.61 chains nm^{-2}, ref 47). Reproduced with permission from ref 85. Copyright 2021 American Chemical Society.

Miscibility. The ability to tune dispersity has potential applications in nanocomposite materials for control over particle dispersion, as for planar surfaces. At high grafting densities, autophobic dewetting can drive polymer-grafted nanoparticles to phase separate from a polymer matrix: for sufficiently long chains, the entropic penalty from the stretching of free and grafting chains dominates over the entropy of mixing.[87] Simulations and theory revealed, however, that highly disperse brushes could stabilize polymer-grafted nanoparticles in polymer melts.[88] When the ratio of the molecular weight of free and grafted polymers $N_{w,f}/N_{w,g}$ is large, high dispersity enhanced steric repulsion (due to interactions between long chains) and, importantly, allowed the matrix chains to penetrate the brush (Figure 7(a,b)). This enhanced wetting eliminated the attractive well that drives grafted nanoparticles to aggregate in melts and solutions. Experiments and self-consistent field theory confirmed that high brush dispersity reduced the attractive interaction (Figure 7(c)) and thereby mitigated the autophobic dewetting for small- to intermediate values of $N_{w,f}/N_{w,g}$.[89] Interestingly, both $N_{w,f}/N_{w,g}$ and Đ appeared to affect the dispersion of PMMA-grafted gold nanoparticles in PMMA matrixes: nanoparticles grafted with polymers of higher Đ remained well dispersed even at relatively high $N_{w,f}/N_{w,g}$ (which favors phase separation of the grafted particles from the matrix) (Figure 7(d,e)).

The molecular weight distribution can also be tuned to control dispersion of polymer-grafted nanoparticles in polymer matrixes when the grafting density is lower. In this limit (allophobic dewetting), the grafted chains do not fully wet the nanoparticle surface and provide incomplete stabilization, leading to nanoparticle aggregation. Using RAFT polymerization in a stepwise fashion enabled separate control over the

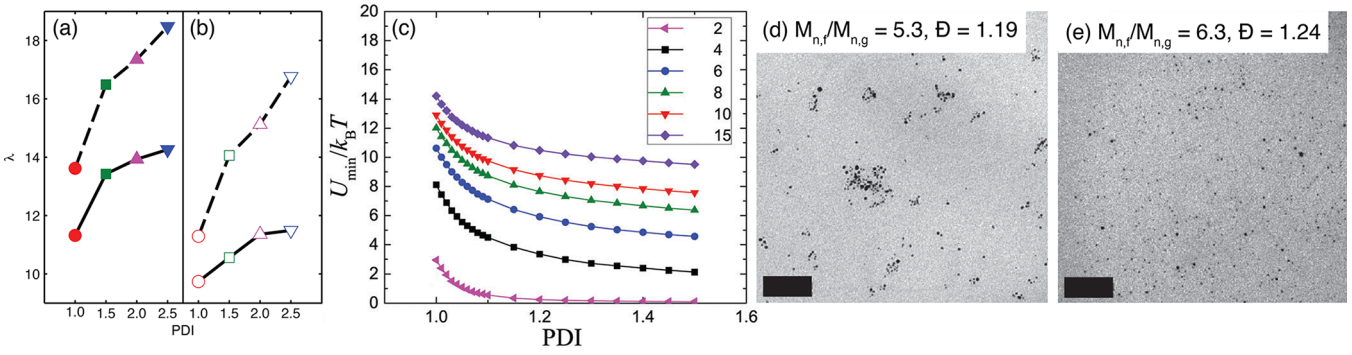

Figure 7. Brush dispersity promotes wetting in homopolymer solutions of polymers. (a, b) Penetration depth λ (in units of the monomer diameter d) of matrix chains into the grafted layer (average degree of polymerization $N_{g,ave}$ = 20) on nanoparticles as a function of Đ for grafting density of 0.10 chains d^{-2} (solid lines) or 0.25 chains d^{-2} (dashed lines) and matrix molecular weights N_{matrix} of (a) 10 and (b) 40. In panels a and b the nanoparticle diameter is $D = 5d$. Panels a and b are reproduced with permission from ref 88. Copyright 2013 American Physical Society. (c) Depth of the potential well U_{min}/k_BT as a function of Đ at various values of the ratio of molecular weight of free and grafted polymers $N_{w,f}/N_{w,g}$ from SCFT; the particle radius is $R = 2aN^{1/2}$ and the brush thickness is $H = 2aN^{1/2}$, where a is the statistical segment length. (d, e) Cross-sectional TEM micrographs of PMMA-functionalized gold nanoparticles in PMMA matrixes; the caption indicates $N_{w,f}/N_{w,g}$ and Đ for the grafted polymer. (d) Grafted molecular weight M_n = 5.3 kDaA, matrix molecular weight M_n = 24 kDa; (e) grafted molecular weight M_n = 11 kDa, matrix molecular weight M_n = 60 kDa. Panels (c) - (e) are reproduced with permission from ref 89. Copyright 2018 Royal Society of Chemistry.

https://doi.org/10.1021/jacsau.2c00638
JACS Au 2023, 3, 333−343

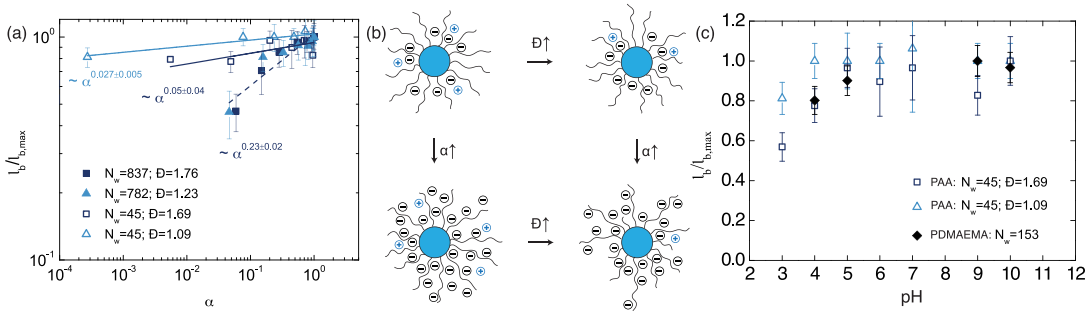

Figure 8. Responsive conformation depends on the molecular weight and dispersity. (a) Normalized brush length $l_b/l_{b,max}$ as a function of degree of dissociation α of the low-N_w PAA brush pair with $N_w = 45$, $Đ = 1.09$ (light blue open triangles) and $N_w = 45$, $Đ = 1.69$ (dark blue open squares) and the high-N_w PAA brush pair with $N_w = 782$, $Đ = 1.23$ (light blue closed triangles) and $N_w = 837$, $Đ = 1.76$ (dark blue closed squares). Solid lines indicate power-law fits for low-N_w brushes, and the dashed line indicates the fit for the high-N_w brushes, which collapsed onto a single curve and were fit together. (b) Schematic illustration of the variation in conformation with $Đ$ and α for the low-N_w brush pair. (c) $l_b/l_{b,max}$ as a function of pH for the low-N_w PAA brush pair compared to a $N_w = 153$ PAA from ref 99. Reproduced with permission from ref 100. Copyright 2021 Royal Society of Chemistry.

composition, molecular weight, and grafting density of two different polymers grafted to nanoparticles.[43] These bimodal surface-grafted brushes can be used to greatly improve dispersion of grafted nanoparticles in polymer matrixes: the short chains provided steric stabilization, whereas the long chains entangled with the matrix polymers.[90] Later synthetic studies advanced the control over the molecular weight of each species and confirmed that the entanglements from even a small fraction of long chains enhanced the toughness of grafted-nanoparticle films.[42]

Self-Assembly. The molecular weight distribution also affects how grafted nanoparticles assemble in polymeric matrixes. Isotropic nanoparticles bearing loosely grafted brushes (such that the cores were able to come into contact) assembled into anisotropic strings.[91] This assembly was determined by a balance between the attractions between the core particles and the elasticity of the grafted polymers. Similarly, nanoparticles bearing loosely grafted disperse PMMA brushes could also self-assemble into string morphologies, driven by the attraction between bare surfaces on the particles.[39] In addition to improving miscibility, bimodal brushes on nanoparticles can also generate a variety of particle assemblies. Nanoparticles bearing long PS polymers and short P2VP polymers self-assembled into vesicle-like structures when the grafting density of PS was low; in this system the short P2VP polymers were thought to reduce the core (particle−particle) attractions and thereby avoid a kinetically trapped nonequilibrium state.[92] Vesicle-like morphologies were also observed for zirconium oxide nanoparticles functionalized with PS and PEO polymers.[93] Thus, dispersity provides an additional parameter by which to modulate the interactions between grafted nanoparticles that drive assembly further or closer to equilibrium.

Stimulus Response. Binary mixed spherical polymer brushes are widely studied as responsive materials, as reviewed in ref 22. Differences in the stimulus response of the two polymers can drive nanoscale segregation of the polymers on the particle surface, leading to changes in wettability or interfacial affinity. In addition to the phase behavior observed for planar surfaces, the ratio of the particle radius of curvature to the polymer radius of gyration can affect the brush morphology under selective solvents. When this ratio is large, the surface appears effectively planar and surface-grafted brushes (e.g., PS−PMMA) could reorganize under selective solvents[94] following theoretical predictions for planar substrates.[95] In P*t*BA-PS mixed brushes, the polymers again exhibited microphase separation in response to selective solvents and the grafting density strongly affected the feature size.[96] When the particle radius of curvature was comparable to the polymer R_g, the density of grafted chains substantially decreased, moving away from the particle surface. Indirect measurements of solvent response (for example, partitioning of PS−PVP cografted gold nanoparticles at the interface of PS and PVP blocks in a copolymer) also suggested that the surface polymers were able to rearrange in response to the solvent conditions.[97]

The effects of continuous dispersity distributions on responsive behavior have been less examined. Homopolymer brushes of stimulus-responsive polymers may show significant differences in their responsive properties depending on the conformation, which in turn should depend on dispersity as well as the molecular weight M_w and grafting density σ. Intriguingly, studies on different polymer brushes produce contrasting results. The normalized length of poly(2-(dimethylamino)ethyl methacrylate) (PDMAEMA) brushes collapsed onto a master curve as a function of pH.[98] By contrast, the pH-dependent length of PAA brushes depended on both brush molecular weight and grafting density.[99] Thus, there remains incomplete understanding of how spherical brush parameters affect the stimulus response.

To address this question, we synthesized annealed brushes of a model weak polyelectrolyte, PAA, and compared the conformation and response of pairs of brushes of near-constant molecular weight but different dispersity.[100] High-dispersity brushes of a relatively low degree of polymerization ($N_w \approx 45$) were longer than low-dispersity brushes; at a higher degree of polymerization ($N_w \approx 813$), however, the length did not substantially change with $Đ$. To understand how the changes in brush conformation were linked to brush charge, we also measured the degree of dissociation α via titration and the zeta potential for each brush pair. Brushes with higher dispersity (compared at constant N_w) or lower molecular weight (compared at constant $Đ$) had higher pK_a values. The zeta potential was more negative (greater magnitude) for higher-$Đ$ brushes (compared at constant N_w) or higher molecular weight brushes (compared at constant $Đ$).

To systematically compare results across brush lengths and charge states, we examined the normalized brush length $l_b/l_{b,max}$ as a function of the degree of dissociation α (Figure 8(a)).[100] For low-N_w brushes ($N_w \approx 45$), the dispersity did not affect the scaling of $l_b/l_{b,max}$ with α (scaling exponent of 0.04), but brushes with lower $Đ$ were more extended at a given α. The very small

https://doi.org/10.1021/jacsau.2c00638
JACS Au 2023, 3, 333−343

scaling exponent indicated that the brush length was insensitive to changes in the degree of dissociation and that brushes were in the quasi-neutral-brush regime, where short-range excluded volume interactions dominate over long-range electrostatic interactions (Figure 8(b)). Indeed, $l_b/l_{b,max}$ of the low-$Đ$ brush was nearly 1, indicating that the excluded volume interactions caused the brush to stretch independent of α. The pH-independent length of the low-N_w, low-$Đ$ PAA brushes was similar to that observed for the N_w = 153 PAA brushes of ref 99 (Figure 8(c)), suggesting that the conformation of these systems was dominated by the excluded volume interactions. For brushes with a high degree of polymerization ($N_w \approx 813$), however, $l_b/l_{b,max}$ for the two brushes fell onto a single curve as a function of α with scaling exponent of 0.23, consistent with a transition in brush conformation from collapsed to stretched as α was increased. Further, the normalized lengths of the PDMAEMA brushes from ref 98 collapsed onto a master curve with those of the high-N_w PAA as a function of pH. Thus, these comparisons suggest that the extent of stimulus response can be tuned through the molecular weight (and length) distribution of the grafted polymers.

CONCLUSIONS AND OUTLOOK

The studies discussed here suggest that tailoring brush dispersity offers a unique route to control the conformation and responsive properties of surface-grafted polymers as summarized in Table 1.

Table 1. Molecular Weight Distribution Used To Tailor Material Properties

context	planar brushes (refs)	spherical brushes (refs)
polymer conformation	48,50−59,62,63	47,83−85
wetting and miscibility	64	43,88−90
segregation	65−70	–
stimulus response	71−74	94,96,99,100
antifouling	78,81,82	–
self-assembly	–	39,92,93

To realize the promise of imparting novel functionality to surfaces by controlling the molecular weight distribution of grafted polymers, we suggest several avenues for further investigations:

- Most current surface-initiated methods to control dispersity are RDRP (such as ATRP or RAFT). Several recently developed methods for tailoring dispersity in solution polymerizations, e.g., using switchable RAFT agents[31,32] or mixing RAFT agents,[30] can likely be adapted to surface-initiated polymerizations but have not yet been demonstrated in this context. Further, little has been explored beyond RDRP methods; ref 47 is a notable exception using ring-opening polymerization to produce surface-grafted polymers of varying dispersity. More synthetic techniques to control the breadth and shape of the distribution applied to surface-initiated polymerizations are needed to open up new properties to be explored.
- Theory and simulation studies are needed to understand how the molecular weight distribution alters polymer conformation, particularly for charged polymers and for spherical brushes (here, building on refs 83, 84, 88). For example, studies of bimodal brushes in which each polymer's molecular weight distribution is narrow (which cannot be experimentally synthesized) or broad (to connect to experiments) are likely to generate clear understanding of the effects of dispersity on brush conformation and (for weak polyelectrolytes) stimulus response, which remains largely unexplored.
- Likewise, detailed experimental studies of the effects of molecular weight distributions on brush conformation are still needed. Atomic force microscopy is widely employed for planar brushes but may not be sufficiently sensitive to capture structural differences arising from tailored dispersity. Neutron scattering methods, including neutron reflectivity for planar brushes[101,102] and small-angle neutron scattering for spherical brushes,[103] offer opportunities to characterize the structure of brushes as a function of the distance from the substrate. Further, the structure of individual components can be isolated through contrast-matching, providing a powerful tool by which to link, e.g., the conformation of a polymer brush to its dispersion in homopolymer matrixes (as one example). Application of these methods to characterize the effects of dispersity on the brush structure is essential for linking the brush structure to the functional properties.
- To date, most work has focused on the effects of dispersity in linear grafted homopolymers. Polymer chemists, however, can create many other polymer architectures. A recent study, for example, showed that increasing the dispersity of the oligomeric side chains in poly(methacrylate)-based comb polymers generated brushes that were more hydrated and less adhesive than those with a more uniform structure.[44] Whether dispersity may affect the properties of other architectures, including bottlebrushes,[104] to our knowledge has not been systematically studied on surfaces, although theorists have begun to develop phase diagrams for bulk melt systems.[105] We anticipate that synthetic methods to controllably generate and characterize brushes of complex architectures will lead to unanticipated responsive properties.
- While our studies described here have provided some insight into the effects of dispersity on pH-response, there are a variety of stimuli that are applied to polymers, including solvent conditions, temperature, and salt concentration and valency (recently characterized for bidisperse polyelectrolyte brushes[106,107]). Additional studies are needed to understand how the molecular weight distribution affects the polymer response to these different stimuli across a range of polymer chemistries.
- Finally, there remains a gap between the many advanced techniques for synthesizing brushes with controlled molecular weight distribution and their use in applications. For example, we anticipate that disperse brushes may exhibit, e.g., unusual mechanical or adhesive properties (the latter suggested by refs 61 and 44) that are distinct from those of uniform brushes, opening new opportunities for applications in sensing, self-assembly, catalysis, nanocomposite processing, and antifouling.

AUTHOR INFORMATION

Corresponding Authors

Jacinta C. Conrad − *William A. Brookshire Department of Chemical and Biomolecular Engineering, University of Houston, Houston, Texas 77204, United States;* orcid.org/0000-0001-6084-4772; Phone: 713-743-3829; Email: jcconrad@uh.edu

Megan L. Robertson − *William A. Brookshire Department of Chemical and Biomolecular Engineering, University of Houston, Houston, Texas 77204, United States;* orcid.org/0000-0002-2903-3733; Phone: 713-743-2748; Email: mlrobertson@uh.edu

https://doi.org/10.1021/jacsau.2c00638
JACS Au 2023, 3, 333−343

Complete contact information is available at:
https://pubs.acs.org/10.1021/jacsau.2c00638

Author Contributions

CRediT: **Jacinta C. Conrad** conceptualization, writing-original draft, writing-review & editing; **Megan L. Robertson** conceptualization, writing-original draft, writing-review & editing.

Notes

The authors declare no competing financial interest.

■ ACKNOWLEDGMENTS

J.C.C. thanks the National Science Foundation (CBET-2113769) and the Welch Foundation (E-1869) for support. M.L.R. thanks the National Science Foundation (DMR-1906009) for support.

■ REFERENCES

(1) Giussi, J. M.; Cortez, M. L.; Marmisollé, W. A.; Azzaroni, O. Practical use of polymer brushes in sustainable energy applications: interfacial nanoarchitectonics for high-efficiency devices. *Chem. Soc. Rev.* **2019**, *48*, 814−849.
(2) Li, D.; Xu, L.; Wang, J.; Gautrot, J. E. Responsive Polymer Brush Design and Emerging Applications for Nanotheranostics. *Adv. Healthcare Mater.* **2021**, *10*, 2000953.
(3) Keating, J. J.; Imbrogno, J.; Belfort, G. Polymer Brushes for Membrane Separations: A Review. *ACS Appl. Mater. Interfaces* **2016**, *8*, 28383−28399.
(4) Zhou, F.; Huck, W. T. S. Three-stage switching of surface wetting using phosphate-bearing polymer brushes. *Chem. Commun.* **2005**, 5999−6001.
(5) Kobayashi, M.; Terayama, Y.; Yamaguchi, H.; Terada, M.; Murakami, D.; Ishihara, K.; Takahara, A. Wettability and Antifouling Behavior on the Surfaces of Superhydrophilic Polymer Brushes. *Langmuir* **2012**, *28*, 7212−7222.
(6) Dunderdale, G. J.; England, M. W.; Urata, C.; Hozumi, A. Polymer Brush Surfaces Showing Superhydrophobicity and Air-Bubble Repellency in a Variety of Organic Liquids. *ACS Appl. Mater. Interfaces* **2015**, *7*, 12220−12229.
(7) Ladd, J.; Zhang, Z.; Chen, S.; Hower, J. C.; Jiang, S. Zwitterionic Polymers Exhibiting High Resistance to Nonspecific Protein Adsorption from Human Serum and Plasma. *Biomacromolecules* **2008**, *9*, 1357−1361.
(8) Zhou, F.; Huck, W. T. S. Surface grafted polymer brushes as ideal building blocks for "smart" surfaces. *Phys. Chem. Chem. Phys.* **2006**, *8*, 3815−3823.
(9) Conrad, J. C.; Robertson, M. L. Towards mimicking biological function with responsive surface-grafted polymer brushes. *Curr. Opin. Solid State Mater. Sci.* **2019**, *23*, 1−12.
(10) Alexander, S. Adsorption of chain molecules with a polar head a scaling description. *J. Phys. (Paris)* **1977**, *38*, 983−987.
(11) de Gennes, P. G. Conformations of Polymers Attached to an Interface. *Macromolecules* **1980**, *13*, 1069−1075.
(12) Dukes, D.; Li, Y.; Lewis, S.; Benicewicz, B.; Schadler, L.; Kumar, S. K. Conformational Transitions of Spherical Polymer Brushes: Synthesis, Characterization, and Theory. *Macromolecules* **2010**, *43*, 1564−1570.
(13) Daoud, M.; Cotton, J. P. Star shaped polymers: a model for the conformation and its concentration dependence. *J. Phys. (Paris)* **1982**, *43*, 531−538.
(14) Birshtein, T. M.; Borisov, O. V.; Zhulina, Y. B.; Khokhlov, A. R.; Yurasova, T. A. Conformations of comb-like macromolecules. *Polymer Science U.S.S.R.* **1987**, *29*, 1293−1300.
(15) Ohno, K.; Morinaga, T.; Takeno, S.; Tsujii, Y.; Fukuda, T. Suspensions of Silica Particles Grafted with Concentrated Polymer Brush: Effects of Graft Chain Length on Brush Layer Thickness and Colloidal Crystallization. *Macromolecules* **2007**, *40*, 9143−9150.
(16) Martinez, A. P.; Carrillo, J.-M. Y.; Dobrynin, A. V.; Adamson, D. H. Distribution of Chains in Polymer Brushes Produced by a "Grafting From" Mechanism. *Macromolecules* **2016**, *49*, 547−553.
(17) Di Landro, L.; Levi, M.; Nichetti, D.; Consolo, A. Experimental determination of rheological properties of polydimethylsiloxane. *Eur. Polym. J.* **2003**, *39*, 1831−1838.
(18) Ye, X.; Sridhar, T. Effects of the Polydispersity on Rheological Properties of Entangled Polystyrene Solutions. *Macromolecules* **2005**, *38*, 3442−3449.
(19) Nielsen, J. K.; Rasmussen, H. K.; Hassager, O.; McKinley, G. H. Elongational viscosity of monodisperse and bidisperse polystyrene melts. *J. Rheol.* **2006**, *50*, 453−476.
(20) Roy, D.; Giller, C. B.; Hogan, T. E.; Roland, C. M. The rheology and gelation of bidisperse 1,4-polybutadiene. *Polymer* **2015**, *81*, 111−118.
(21) Nadgorny, M.; Gentekos, D. T.; Xiao, Z.; Singleton, S. P.; Fors, B. P.; Connal, L. A. Manipulation of Molecular Weight Distribution Shape as a New Strategy to Control Processing Parameters. *Macromol. Rapid Commun.* **2017**, *38*, 1700352.
(22) Zhao, B.; Zhu, L. Mixed Polymer Brush-Grafted Particles: A New Class of Environmentally Responsive Nanostructured Materials. *Macromolecules* **2009**, *42*, 9369−9383.
(23) Li, M.; Pester, C. W. Mixed Polymer Brushes for "Smart" Surfaces. *Polymers* **2020**, *12*, 1553.
(24) Gentekos, D. T.; Dupuis, L. N.; Fors, B. P. Beyond Dispersity: Deterministic Control of Polymer Molecular Weight Distribution. *J. Am. Chem. Soc.* **2016**, *138*, 1848−1851.
(25) Li, H.; Collins, C. R.; Ribelli, T. G.; Matyjaszewski, K.; Gordon, G. J.; Kowalewski, T.; Yaron, D. J. Tuning the molecular weight distribution from atom transfer radical polymerization using deep reinforcement learning. *Molecular Systems Design & Engineering* **2018**, *3*, 496−508.
(26) Gentekos, D. T.; Sifri, R. J.; Fors, B. P. Controlling polymer properties through the shape of the molecular-weight distribution. *Nature Review Materials* **2019**, *4*, 761−774.
(27) Whitfield, R.; Truong, N. P.; Messmer, D.; Parkatzidis, K.; Rolland, M.; Anastasaki, A. Tailoring polymer dispersity and shape of molecular weight distributions: methods and applications. *Chemical Science* **2019**, *10*, 8724−8734.
(28) Junkers, T. Polymers in the Blender. *Macromol. Chem. Phys.* **2020**, *221*, 2000234.
(29) Walsh, D. J.; Schinski, D. A.; Schneider, R. A.; Guironnet, D. General route to design polymer molecular weight distributions through flow chemistry. *Nat. Commun.* **2020**, *11*, 3094.
(30) Whitfield, R.; Parkatzidis, K.; Truong, N. P.; Junkers, T.; Anastasaki, A. Tailoring Polymer Dispersity by RAFT Polymerization: A Versatile Approach. *Chem.* **2020**, *6*, 1340−1352.
(31) Antonopoulou, M.-H.; Whitfield, R.; Truong, N. P.; Wyers, D.; Harrisson, S.; Junkers, T.; Anastasaki, A. Concurrent control over sequence and dispersity in multiblock copolymers. *Nat. Chem.* **2022**, *14*, 304−312.
(32) Antonopoulou, M.-N.; Whitfield, R.; Truong, N. P.; Anastasaki, A. Controlling polymer dispersity using switchable RAFT agents: Unravelling the effect of the organic content and degree of polymerization. *Eur. Polym. J.* **2022**, *174*, 111326.
(33) Whitfield, R.; Truong, N. P.; Anastasaki, A. Precise Control of Both Dispersity and Molecular Weight Distribution Shape by Polymer Blending. *Angew. Chem., Int. Ed.* **2021**, *60*, 19383−19388.
(34) Zoppe, J. O.; Ataman, N. C.; Mocny, P.; Wang, J.; Moraes, J.; Klok, H.-A. Surface-Initiated Controlled Radical Polymerization: State-of-the-Art, Opportunities, and Challenges in Surface and Interface Engineering with Polymer Brushes. *Chem. Rev.* **2017**, *117*, 1105−1318.
(35) Yin, R.; Wang, Z.; Bockstaller, M. R.; Matyjaszewski, K. Tuning dispersity of linear polymers and polymeric brushes grown from nanoparticles by atom transfer radical polymerization. *Polym. Chem.* **2021**, *12*, 6071−6082.
(36) Pester, C. W.; Benetti, E. M. Modulation of Polymer Brush Properties by Tuning Dispersity. *Advanced Materials Interfaces* **2022**, *9*, 2201439.

(37) Chen, W.-L.; Cordero, R.; Tran, H.; Ober, C. K. 50th Anniversary Perspective: Polymer Brushes: Novel Surfaces for Future Materials. *Macromolecules* **2017**, *50*, 4089−4113.
(38) Hansson, S.; Trouillet, V.; Tischer, T.; Goldmann, A. S.; Carlmark, A.; Barner-Kowollik, C.; Malmström, E. Grafting Efficiency of Synthetic Polymers onto Biomaterials: A Comparative Study of Grafting-from versus Grafting-to. *Biomacromolecules* **2013**, *14*, 64−74.
(39) Wang, Z.; Yan, J.; Liu, T.; Wei, Q.; Li, S.; Olszewski, M.; Wu, J.; Sobieski, J.; Fantin, M.; Bockstaller, M. R.; Matyjaszewski, K. Control of Dispersity and Grafting Density of Particle Brushes by Variation of ATRP Catalyst Concentration. *ACS Macro Lett.* **2019**, *8*, 859−864.
(40) Wang, Z.; Fantin, M.; Sobieski, J.; Wang, Z.; Yan, J.; Lee, J.; Liu, T.; Li, S.; Olszewski, M.; Bockstaller, M. R.; Matyjaszewski, K. Pushing the Limit: Synthesis of SiO2-g-PMMA/PS Particle Brushes via ATRP with Very Low Concentration of Functionalized SiO2−Br Nanoparticles. *Macromolecules* **2019**, *52*, 8713−8723.
(41) Yadav, V.; Hashmi, N.; Ding, W.; Li, T.-H.; Mahanthappa, M. K.; Conrad, J. C.; Robertson, M. L. Dispersity control in atom transfer radical polymerizations through addition of phenylhydrazine. *Polym. Chem.* **2018**, *9*, 4332−4342.
(42) Yan, J.; Kristufek, T.; Schmitt, M.; Wang, Z.; Xie, G.; Dang, A.; Hui, C. M.; Pietrasik, J.; Bockstaller, M. R.; Matyjaszewski, K. Matrix-free Particle Brush System with Bimodal Molecular Weight Distribution Prepared by SI-ATRP. *Macromolecules* **2015**, *48*, 8208−8218.
(43) Rungta, A.; Natarajan, B.; Neely, T.; Dukes, D.; Schadler, L. S.; Benicewicz, B. C. Grafting Bimodal Polymer Brushes on Nanoparticles Using Controlled Radical Polymerization. *Macromolecules* **2012**, *45*, 9303−9311.
(44) Romio, M.; Grob, B.; Trachsel, L.; Mattarei, A.; Morgese, G.; Ramakrishna, S. N.; Niccolai, F.; Guazzelli, E.; Paradisi, C.; Martinelli, E.; Spencer, N. D.; Benetti, E. M. Dispersity within Brushes Plays a Major Role in Determining Their Interfacial Properties: The Case of Oligoxazoline-Based Graft Polymers. *J. Am. Chem. Soc.* **2021**, *143*, 19067−19077.
(45) Liu, X.; Wang, C.; Goto, A. Polymer Dispersity Control by Organocatalyzed Living Radical Polymerization. *Angew. Chem., Int. Ed.* **2019**, *58*, 5598−5603.
(46) Wang, C.-G.; Chong, A. M. L.; Goto, A. One Reagent with Two Functions: Simultaneous Living Radical Polymerization and Chain-End Substitution for Tailoring Polymer Dispersity. *ACS Macro Lett.* **2021**, *10*, 584−590.
(47) Bentz, K. C.; Savin, D. A. Chain Dispersity Effects on Brush Properties of Surface-Grafted Polycaprolactone-Modified Silica Nanoparticles: Unique Scaling Behavior in the Concentrated Polymer Brush Regime. *Macromolecules* **2017**, *50*, 5565−5573.
(48) Milner, S. T.; Witten, T. A.; Cates, M. E. Effects of polydispersity in the end-grafted polymer brush. *Macromolecules* **1989**, *22*, 853−861.
(49) Qi, S.; Klushin, L. I.; Skvortsov, A. M.; Schmid, F. Polydisperse Polymer Brushes: Internal Structure, Critical Behavior, and Interaction with Flow. *Macromolecules* **2016**, *49*, 9665−9683.
(50) Birshtein, T.; Liatskaya, Y.; Zhulina, E. Theory of supermolecular structures of polydisperse block copolymers: 1. Planar layers of grafted chains. *Polymer* **1990**, *31*, 2185−2196.
(51) Dan, N.; Tirrell, M. Effect of bimodal molecular weight distribution on the polymer brush. *Macromolecules* **1993**, *26*, 6467−6473.
(52) de Vos, W. M.; Leermakers, F. A. M. Modeling the structure of a polydisperse polymer brush. *Polymer* **2009**, *50*, 305−316.
(53) Chakrabarti, A.; Toral, R. Density profile of terminally anchored polymer chains: a Monte Carlo study. *Macromolecules* **1990**, *23*, 2016−2021.
(54) Lai, P. Y.; Zhulina, E. B. Structure of a bidisperse polymer brush: Monte Carlo simulation and self-consistent field results. *Macromolecules* **1992**, *25*, 5201−5207.
(55) Kent, M. S.; Factor, B. J.; Satija, S.; Gallagher, P.; Smith, G. S. Structure of Bimodal Polymer Brushes in a Good Solvent by Neutron Reflectivity. *Macromolecules* **1996**, *29*, 2843−2849.
(56) Kritikos, G.; Terzis, A. F. Structure of bimodal and polydisperse polymer brushes in a good solvent studied by numerical mean field theory. *Polymer* **2005**, *46*, 8355−8365.
(57) Levicky, R.; Koneripalli, N.; Tirrell, M.; Satija, S. K. Stratification in Bidisperse Polymer Brushes from Neutron Reflectivity. *Macromolecules* **1998**, *31*, 2616−2621.
(58) Goedel, W. A.; Luap, C.; Oeser, R.; Lang, P.; Braun, C.; Steitz, R. Stratification in Monolayers of a Bidisperse Melt Polymer Brush As Revealed by Neutron Reflectivity. *Macromolecules* **1999**, *32*, 7599−7609.
(59) Terzis, A. F. Bidisperse melt polymer brush studied by self-consistent field model. *Polymer* **2002**, *43*, 2435−2444.
(60) Reiter, G.; Auroy, P.; Auvray, L. Instabilities of Thin Polymer Films on Layers of Chemically Identical Grafted Molecules. *Macromolecules* **1996**, *29*, 2150−2157.
(61) Reiter, G.; Schultz, J.; Auroy, P.; Auvray, L. Improving adhesion via connector polymers to stabilize non-wetting liquid films. *Europhys. Lett.* **1996**, *33*, 29−34.
(62) Witten, T. A.; Milner, S. T. Two-Component Grafted Polymer Layers. *MRS Online Proceedings Library* **1989**, *177*, 37−45.
(63) Lai, P. Binary mixture of grafted polymer chains: A Monte Carlo simulation. *J. Chem. Phys.* **1994**, *100*, 3351−3357.
(64) Edgecombe, S. R.; Gardiner, J. M.; Matsen, M. W. Suppressing Autophobic Dewetting by Using a Bimodal Brush. *Macromolecules* **2002**, *35*, 6475−6477.
(65) Marko, J. F.; Witten, T. A. Phase separation in a grafted polymer layer. *Phys. Rev. Lett.* **1991**, *66*, 1541−1544.
(66) Müller, M. Phase diagram of a mixed polymer brush. *Phys. Rev. E* **2002**, *65*, 030802.
(67) Wang, J.; Müller, M. Microphase Separation of Mixed Polymer Brushes: Dependence of the Morphology on Grafting Density, Composition, Chain-Length Asymmetry, Solvent Quality, and Selectivity. *J. Phys. Chem. B* **2009**, *113*, 11384−11402.
(68) Minko, S.; Luzinov, I.; Luchnikov, V.; Müller, M.; Patil, S.; Stamm, M. Bidisperse Mixed Brushes: Synthesis and Study of Segregation in Selective Solvent. *Macromolecules* **2003**, *36*, 7268−7279.
(69) Estillore, N. C.; Advincula, R. C. Stimuli-Responsive Binary Mixed Polymer Brushes and Free-Standing Films by LbL-SIP. *Langmuir* **2011**, *27*, 5997−6008.
(70) Wei, W.; Kim, T.-Y.; Balamurugan, A.; Sun, J.; Chen, R.; Ghosh, A.; Rodolakis, F.; McChesney, J. L.; Lakkham, A.; Evans, P. G.; Hur, S.-M.; Gopalan, P. Phase Behavior of Mixed Polymer Brushes Grown from Ultrathin Coatings. *ACS Macro Lett.* **2019**, *8*, 1086−1090.
(71) Houbenov, N.; Minko, S.; Stamm, M. Mixed Polyelectrolyte Brush from Oppositely Charged Polymers for Switching of Surface Charge and Composition in Aqueous Environment. *Macromolecules* **2003**, *36*, 5897−5901.
(72) Delcroix, M. F.; Huet, G. L.; Conard, T.; Demoustier-Champagne, S.; Du Prez, F. E.; Landoulsi, J.; Dupont-Gillain, C. C. Design of Mixed PEO/PAA Brushes with Switchable Properties Toward Protein Adsorption. *Biomacromolecules* **2013**, *14*, 215−225.
(73) Bratek-Skicki, A.; Eloy, P.; Morga, M.; Dupont-Gillain, C. Reversible Protein Adsorption on Mixed PEO/PAA Polymer Brushes: Role of Ionic Strength and PEO Content. *Langmuir* **2018**, *34*, 3037−3048.
(74) Yadav, V.; Harkin, A. V.; Robertson, M. L.; Conrad, J. C. Hysteretic memory in pH-response of water contact angle on poly(acrylic acid) brushes. *Soft Matter* **2016**, *12*, 3589−3599.
(75) Aulich, D.; Hoy, O.; Luzinov, I.; Brücher, M.; Hergenröder, R.; Bittrich, E.; Eichhorn, K.-J.; Uhlmann, P.; Stamm, M.; Esser, N.; Hinrichs, K. In Situ Studies on the Switching Behavior of Ultrathin Poly(acrylic acid) Polyelectrolyte Brushes in Different Aqueous Environments. *Langmuir* **2010**, *26*, 12926−12932.
(76) Weidman, J. L.; Mulvenna, R. A.; Boudouris, B. W.; Phillip, W. A. Unusually Stable Hysteresis in the pH-Response of Poly(Acrylic Acid) Brushes Confined within Nanoporous Block Polymer Thin Films. *J. Am. Chem. Soc.* **2016**, *138*, 7030−7039.

https://doi.org/10.1021/jacsau.2c00638
JACS Au 2023, 3, 333−343

(77) Dong, R.; Lindau, M.; Ober, C. K. Dissociation Behavior of Weak Polyelectrolyte Brushes on a Planar Surface. *Langmuir* **2009**, *25*, 4774−4779.
(78) de Vos, W. M.; Leermakers, F. A. M.; de Keizer, A.; Kleijn, J. M.; Cohen Stuart, M. A. Interaction of Particles with a Polydisperse Brush: A Self-Consistent-Field Analysis. *Macromolecules* **2009**, *42*, 5881−5891.
(79) Badoux, M.; Billing, M.; Klok, H.-A. Polymer brush interfaces for protein biosensing prepared by surface-initiated controlled radical polymerization. *Polym. Chem.* **2019**, *10*, 2925−2951.
(80) Lau, K. H. A.; Ren, C.; Park, S. H.; Szleifer, I.; Messersmith, P. B. An Experimental−Theoretical Analysis of Protein Adsorption on Peptidomimetic Polymer Brushes. *Langmuir* **2012**, *28*, 2288−2298.
(81) Bosker, W. T. E.; Iakovlev, P. A.; Norde, W.; Cohen Stuart, M. A. BSA adsorption on bimodal PEO brushes. *J. Colloid Interface Sci.* **2005**, *286*, 496−503.
(82) Yadav, V.; Jaimes-Lizcano, Y. A.; Dewangan, N. K.; Park, N.; Li, T.-H.; Robertson, M. L.; Conrad, J. C. Tuning Bacterial Attachment and Detachment via the Thickness and Dispersity of a pH-Responsive Polymer Brush. *ACS Appl. Mater. Interfaces* **2017**, *9*, 44900−44910.
(83) Nair, N.; Wentzel, N.; Jayaraman, A. Effect of bidispersity in grafted chain length on grafted chain conformations and potential of mean force between polymer grafted nanoparticles in a homopolymer matrix. *J. Chem. Phys.* **2011**, *134*, 194906.
(84) Dodd, P. M.; Jayaraman, A. Monte Carlo simulations of polydisperse polymers grafted on spherical surfaces. *J. Polym. Sci., Part B: Polym. Phys.* **2012**, *50*, 694−705.
(85) Li, T.-H.; Yadav, V.; Conrad, J. C.; Robertson, M. L. Effect of Dispersity on the Conformation of Spherical Polymer Brushes. *ACS Macro Lett.* **2021**, *10*, 518−524.
(86) Petroff, M. G.; Garcia, E. A.; Dengler, R. A.; Herrera-Alonso, M.; Bevan, M. A. *kT*-Scale Interactions and Stability of Colloids with Adsorbed Zwitterionic and Ethylene Oxide Copolymers. *Macromolecules* **2018**, *51*, 9156−9164.
(87) Koh, C.; Grest, G. S.; Kumar, S. K. Assembly of Polymer-Grafted Nanoparticles in Polymer Matrices. *ACS Nano* **2020**, *14*, 13491−13499.
(88) Martin, T. B.; Dodd, P. M.; Jayaraman, A. Polydispersity for Tuning the Potential of Mean Force between Polymer Grafted Nanoparticles in a Polymer Matrix. *Phys. Rev. Lett.* **2013**, *110*, 018301.
(89) Park, S. J.; Kim, S.; Yong, D.; Choe, Y.; Bang, J.; Kim, J. U. Interactions between brush-grafted nanoparticles within chemically identical homopolymers: the effect of brush polydispersity. *Soft Matter* **2018**, *14*, 1026−1042.
(90) Li, Y.; Tao, P.; Viswanath, A.; Benicewicz, B. C.; Schadler, L. S. Bimodal Surface Ligand Engineering: The Key to Tunable Nanocomposites. *Langmuir* **2013**, *29*, 1211−1220.
(91) Akcora, P.; Liu, H.; Kumar, S. K.; Moll, J.; Li, Y.; Benicewicz, B. C.; Schadler, L. S.; Acehan, D.; Panagiotopoulos, A. Z.; Pryamitsyn, V.; Ganesan, V.; Ilavsky, J.; Thiyagarajan, P.; Colby, R. H.; Douglas, J. F. Anisotropic self-assembly of spherical polymer-grafted nanoparticles. *Nat. Mater.* **2009**, *8*, 354−359.
(92) Zhao, D.; Di Nicola, M.; Khani, M. M.; Jestin, J.; Benicewicz, B. C.; Kumar, S. K. Self-Assembly of Monodisperse versus Bidisperse Polymer-Grafted Nanoparticles. *ACS Macro Lett.* **2016**, *5*, 790−795.
(93) Guzman-Juarez, B.; Abdelaal, A.; Kim, K.; Toader, V.; Reven, L. Fabrication of Amphiphilic Nanoparticles via Mixed Homopolymer Brushes and NMR Characterization of Surface Phase Separation. *Macromolecules* **2018**, *51*, 9951−9960.
(94) Li, D.; Sheng, X.; Zhao, B. Environmentally Responsive "Hairy" Nanoparticles: Mixed Homopolymer Brushes on Silica Nanoparticles Synthesized by Living Radical Polymerization Techniques. *J. Am. Chem. Soc.* **2005**, *127*, 6248−6256.
(95) Zhao, B.; Zhu, L. Nanoscale Phase Separation in Mixed Poly(*tert*-butyl acrylate)/Polystyrene Brushes on Silica Nanoparticles under Equilibrium Melt Conditions. *J. Am. Chem. Soc.* **2006**, *128*, 4574−4575.
(96) Jiang, X.; Zhao, B.; Zhong, G.; Jin, N.; Horton, J. M.; Zhu, L.; Hafner, R. S.; Lodge, T. P. Microphase Separation of High Grafting Density Asymmetric Mixed Homopolymer Brushes on Silica Particles. *Macromolecules* **2010**, *43*, 8209−8217.
(97) Chiu, J. J.; Kim, B. J.; Kramer, E. J.; Pine, D. J. Control of Nanoparticle Location in Block Copolymers. *J. Am. Chem. Soc.* **2005**, *127*, 5036−5037.
(98) Iqbal, D.; Yan, J.; Matyjaszewski, K.; Tilton, R. D. Swelling of multi-responsive spherical polyelectrolyte brushes across a wide range of grafting densities. *Colloid Polym. Sci.* **2020**, *298*, 35−49.
(99) Zhang, C.; Carlson, T.; Yang, S.; Akcora, P. Ordering pH-Responsive Polyelectrolyte-Grafted Nanoparticles in a Flow Coating Process. *Advanced Materials Interfaces* **2018**, *5*, 1701318.
(100) Li, T.-H.; Robertson, M. L.; Conrad, J. C. Molecular weight and dispersity affect chain conformation and pH-response in weak polyelectrolyte brushes. *Polym. Chem.* **2021**, *12*, 6737−6744.
(101) Field, J. B.; Toprakcioglu, C.; Ball, R. C.; Stanley, H. B.; Dai, L.; Barford, W.; Penfold, J.; Smith, G.; Hamilton, W. Determination of end-adsorbed polymer density profiles by neutron reflectometry. *Macromolecules* **1992**, *25*, 434−439.
(102) Kilbey, S. M.; Ankner, J. F. Neutron reflectivity as a tool to understand polyelectrolyte brushes. *Curr. Opin. Colloid Interface Sci.* **2012**, *17*, 83−89.
(103) Wei, Y.; Hore, M. J. A. Characterizing polymer structure with small-angle neutron scattering: A Tutorial. *J. Appl. Phys.* **2021**, *129*, 171101.
(104) Verduzco, R.; Li, X.; Pesek, S. L.; Stein, G. E. Structure, function, self-assembly, and applications of bottlebrush copolymers. *Chem. Soc. Rev.* **2015**, *44*, 2405−2420.
(105) Starvaggi, H.; Tian, Y.; Liang, H.; Dobrynin, A. V. Bottlebrushes and Combs with Bimodal Distribution of the Side Chains: Diagram of States and Scattering Function. *Macromolecules* **2021**, *54*, 1818−1828.
(106) Li, Y.; Hao, Q.-H.; Xia, S.-Y.; Yan, D.-X.; Tan, H.-G. Morphologies of spherical bidisperse polyelectrolyte brushes in the presence of trivalent counterions. *Chem. Phys.* **2020**, *539*, 110941.
(107) Hao, Q.-H.; Cheng, J. Morphologies of a spherical bimodal polyelectrolyte brush induced by polydispersity and solvent selectivity. *Chinese Physics B* **2021**, *30*, 068201.

https://doi.org/10.1021/jacsau.2c00638
JACS Au 2023, 3, 333−343